PRAMANA — journal of physics

Vol. 79, No. 5
November 2012
pp. 979–992

Neutrino mass and mixing – status

THOMAS SCHWETZ
Max-Planck-Institut für Kernphysik, Saupfercheckweg 1, 69117 Heidelberg, Germany
E-mail: schwetz@mpi-hd.mpg.de

Abstract. The status of neutrino oscillations from global data are summarized. An update on the three-flavour picture and recent developments are discussed with regard to the measurement of the mixing angle θ_{13}. Global data currently provide an indication at 3σ that θ_{13} is non-zero. Furthermore, the status of sterile neutrino oscillation interpretations of the LSND anomaly in the light of MiniBooNE results and a recent re-evaluation of the neutrino fluxes from nuclear reactors are discussed. Despite several hints for sterile neutrinos at the eV scale, there is severe tension in the global data and no consistent description of all data is possible.

Keyword. Neutrino oscillations.

PACS Nos 14.60.Lm; 14.60.Pq; 14.60.St

1. Introduction

Experimental results accumulated over the last 12 years provide convincing evidence for neutrino oscillations. This implies that at least two out of the three neutrinos in the Standard Model (SM) have non-zero mass. In the presence of a mass term for neutrinos, one expects that the neutrino fields participating in the charged current (CC) interaction, will be superpositions of the fields with definite mass. Hence, there will be mixing in the lepton sector, in the same way as CKM mixing in the quark sector. Let us consider, to be specific, a Majorana mass term for neutrinos, together with the mass term for charged leptons:

$$\mathcal{L}_{\rm M} = -\frac{1}{2}\sum_{i=1}^{3} \nu_{i\rm L}^T C^{-1} \nu_{i\rm L} m_i^\nu - \sum_{\alpha=e,\mu,\tau} \bar{\ell}_{\alpha\rm R}\ell_{\alpha\rm L} m_\alpha^\ell + \text{h.c.} \tag{1}$$

Then in general the CC interaction is not diagonal on the basis of the neutrino mass eigenfields ν_1, ν_2, ν_3, used in eq. (1):

$$\mathcal{L}_{\rm CC} = -\frac{g}{\sqrt{2}} W^\rho \sum_{\alpha=e,\mu,\tau} \sum_{i=1}^{3} \bar{\nu}_{i\rm L} U_{\alpha i}^* \gamma_\rho \ell_{\alpha\rm L} + \text{h.c.}, \tag{2}$$

DOI: 10.1007/s12043-012-0414-2; ***e*Publication: 27 October 2012**

where $(U_{\alpha i}) \equiv U_{\rm PMNS}$ is the Pontecorvo–Maki–Nakagawa–Sakata lepton mixing matrix [1]. Note that the 'effective' mass term in eq. (1) violates gauge invariance. Therefore, the SM has to be extended in order to give mass to neutrinos in a consistent way. In particular, it is necessary to add new degrees of freedom to the SM, such as right-handed neutrinos or new scalar representations.

The conventional parametrization [2] for the lepton mixing matrix is $U_{\rm PMNS} = V^{\rm Dirac} D^{\rm Maj}$, with

$$V^{\rm Dirac} = \begin{pmatrix} 1 & 0 & 0 \\ 0 & c_{23} & s_{23} \\ 0 & -s_{23} & c_{23} \end{pmatrix} \begin{pmatrix} c_{13} & 0 & \mathrm{e}^{-i\delta} s_{13} \\ 0 & 1 & 0 \\ -\mathrm{e}^{i\delta} s_{13} & 0 & c_{13} \end{pmatrix} \begin{pmatrix} c_{12} & s_{12} & 0 \\ -s_{12} & c_{12} & 0 \\ 0 & 0 & 1 \end{pmatrix}, \tag{3}$$

where $s_{ij} \equiv \sin\theta_{ij}$ and $c_{ij} \equiv \cos\theta_{ij}$. The three mixing angles are given by

$$\tan\theta_{23} = \frac{|U_{\mu 3}|}{|U_{\tau 3}|}, \qquad \sin\theta_{13} = |U_{e3}|, \qquad \tan\theta_{12} = \frac{|U_{e2}|}{|U_{e1}|}. \tag{4}$$

There is one Dirac phase δ which leads to CP-violation in neutrino oscillations. Furthermore, if neutrinos are Majorana particles there are two physical Majorana phases in $D^{\rm Maj} \equiv \mathrm{diag}(1, \mathrm{e}^{i\alpha/2}, \mathrm{e}^{i\beta/2})$, which have no effect in neutrino oscillations, but appear in lepton-number violating processes such as neutrinoless double beta decay (see [3]).

2. Global three-flavour analysis

Thanks to the spectacular developments in neutrino oscillation experiments in the previous decade we have now a rough picture of the parameters governing three-flavour oscillations: There are two mass-squared differences separated roughly by a factor 30, there are two large mixing angles (θ_{23}, which could even be 45°, and θ_{12}, which is large but smaller than 45° at very high significance), and one mixing angle which has to be small (θ_{13}). Present data are consistent with two possibilities for the neutrino mass ordering, conventionally parametrized by the sign of Δm^2_{31}: In the normal ordering ($\Delta m^2_{31} > 0$), the mass state which contains predominantly the electron neutrino has the smallest mass, whereas in the inverted ordering ($\Delta m^2_{31} < 0$), it is part of a nearly degenerate doublet of mass states which is separated from the lightest neutrino mass by $|\Delta m^2_{31}|$. The basic picture is summarized in figure 1.

In the following, an update is presented on the determination of three-neutrino oscillation parameters from a global analysis of the latest world neutrino oscillation data from solar, atmospheric, reactor, and accelerator experiments. These results are based on work in collaboration with Tortola and Valle, published in refs [4–6]. The present determination of the three-flavour oscillation parameters is summarized in table 1, where the best-fit points and the 2σ and 3σ allowed ranges are given.

The determination the parameters responsible for the leading oscillation modes is illustrated in figure 2. It shows the complemetarity of natural (solar and atmospheric) and artificial (reactors and accelerators) neutrino sources. The KamLAND reactor

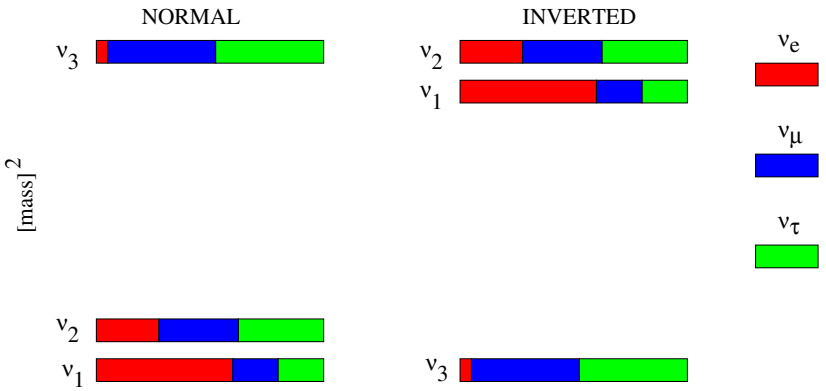

Figure 1. Schematic picture of neutrino mass and mixing as determined from oscillation data. The left and right graphs correspond to normal and inverted neutrino mass ordering, respectively.

experiment observes a spectral distortion of the neutrino survival probability at the 5σ level [7], consistent with the L/E dependence expected from oscillations, where L is the distance between neutrino source and detector and E is the neutrino energy. In addition to being the smoking gun signature for neutrino oscillations, this provides the very accurate determination of Δm^2_{21}. The determination of $|\Delta m^2_{31}|$ is dominated by the energy-dependent ν_μ disappearance observed in the MINOS long-baseline experiment [8,9].

Table 1. Summary of neutrino oscillation parameters. For Δm^2_{31}, $\sin^2\theta_{23}$, $\sin^2\theta_{13}$, and δ the upper and lower rows correspond to normal and inverted neutrino mass hierarchy, respectively (see refs [5,6] for details and references).

Parameter	Best fit $\pm 1\sigma$	2σ	3σ
Δm^2_{21} (10^{-5} eV^2)	$7.59^{+0.20}_{-0.18}$	7.24–7.99	7.09–8.19
Δm^2_{31} (10^{-3} eV^2)	$2.50^{+0.09}_{-0.16}$	2.25–2.68	2.14–2.76
	$-(2.40^{+0.08}_{-0.09})$	$-$(2.23–2.58)	$-$(2.13–2.67)
$\sin^2\theta_{12}$	$0.312^{+0.017}_{-0.015}$	0.28–0.35	0.27–0.36
$\sin^2\theta_{23}$	$0.52^{+0.06}_{-0.07}$	0.41–0.61	0.39–0.64
	0.52 ± 0.06	0.42–0.61	
$\sin^2\theta_{13}$	$0.013^{+0.007}_{-0.005}$	0.004–0.028	0.001–0.035
	$0.016^{+0.008}_{-0.006}$	0.005–0.031	0.001–0.039
δ	$\left(-0.61^{+0.75}_{-0.65}\right)\pi$	0–2π	0–2π
	$\left(-0.41^{+0.65}_{-0.70}\right)\pi$		

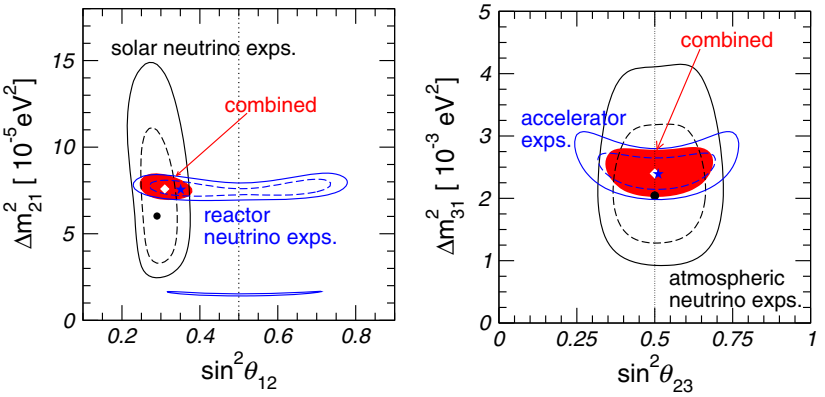

Figure 2. Determination of oscillation parameters for leading oscillation modes from the interplay of global data [4].

3. Status of θ_{13}

Up to June 2011, the information on the mixing angle θ_{13} was dominated by the upper bound from the CHOOZ reactor experiment [10], with a weak indication of $\theta_{13} > 0$ from the global data, at the 1.5σ level (see e.g., [5]). Recently, the T2K and Double-Chooz experiments announced first results of their search for this mixing angle and those developements are reported here.

The T2K experiment uses a neutrino beam consisting mainly of muon neutrinos, produced at the J-PARC Accelerator Facility and observed at a distance of 295 km and an off-axis angle of 2.5° by the Super-Kamiokande detector. The present data release corresponds to 1.43×10^{20} protons on target [11,12]. Six events pass all selection criteria for an electron neutrino event. In a three-flavour neutrino oscillation scenario with $\theta_{13} = 0$, the expected number of such events is 1.5 ± 0.3(syst). Under this hypothesis, the probability to observe six or more candidate events is 7×10^{-3}, equivalent to a significance of 2.5σ. Latest MINOS data on the $\nu_\mu \to \nu_e$ channel are presented in refs [8,13], corresponding to 8.2×10^{20} protons on target. MINOS finds 62 events with an expectation in the absence of oscillations of 49.6 ± 7.0(stat) ± 2.7(syst), showing no significant indication for $\nu_\mu \to \nu_e$ transitions. In figure 3 we show the region in the $\sin^2\theta_{13}$–δ plane indicated by T2K data in comparison with MINOS results. While for T2K we obtain a closed region for $\sin^2\theta_{13}$ at $\Delta\chi^2 = 2.7$, for MINOS we find only an upper bound. The results are clearly compatible and we show the combined analysis as shaded regions, where the upper bound is determined by the MINOS constraint while the lower bound is given by T2K. Best-fit values are in the range $\sin^2\theta_{13} \approx 0.015 - 0.023$, depending on the CP phase δ, where the variation is somewhat larger for the inverted mass hierarchy. The dotted lines in the figure indicate the 90% CL upper bound on $\sin^2\theta_{13}$ coming from a combined analysis of the remaining oscillation data, including global reactor, solar, atmospheric, and long-baseline disappearance data.

We move now to the combined analysis of the T2K and MINOS ν_e appearance searches with global neutrino oscillation data as described and referenced in ref. [5]. The results

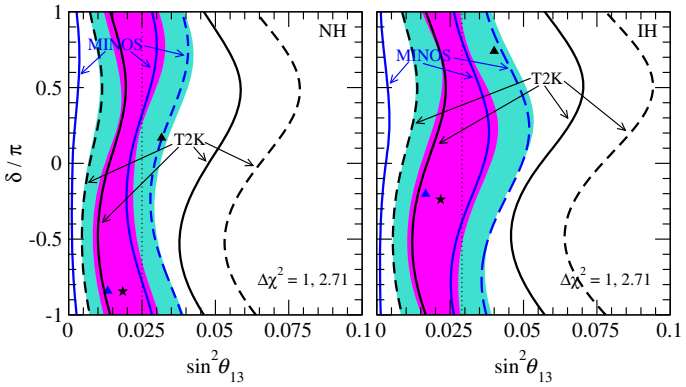

Figure 3. Contours of $\Delta\chi^2 = 1, 2.71$ for T2K and MINOS appearance data (curves) and their combination (shaded regions). For all other oscillation parameters best-fit values and uncertainties are assumed and according to table 1, a 5% uncertainty is included on the matter density. The left and right panels are for normal and inverted mass hierarchy, respectively. The dotted line shows the 90% CL upper limit on $\sin^2\theta_{13}$ from a combined analysis of all other oscillation data. The blue (black) triangle corresponds to the best-fit point of the MINOS (T2K) data analysis, while the black star denotes the best-fit point of the combined MINOS + T2K analysis.

for θ_{13} are summarized in figure 4. For both neutrino mass hierarchies we find that the 2.5σ indication for $\theta_{13} > 0$ from T2K gets pushed to the 3σ level ($\Delta\chi^2 = 9$) when combined with the weak hint for a non-zero θ_{13} obtained from the remaining data [5]. We find best-fit points at

$$\sin^2\theta_{13} = 0.013\,, \quad \delta = -0.61\pi \qquad \text{(normal hierarchy)},$$
$$\sin^2\theta_{13} = 0.016\,, \quad \delta = -0.41\pi \qquad \text{(inverted hierarchy)}. \tag{5}$$

Due to some complementarity between T2K and MINOS one obtains, after combining with the θ_{13} limit from the rest of the data, a 'preferred region' for the CP phase δ at $\Delta\chi^2 = 1$, as seen in figure 4. Obviously this preference for the CP phase is not significant [13a]. Marginalizing over the CP phase δ (and all other oscillation parameters) we obtain for the best-fit, 1σ errors, and the significance for $\theta_{13} > 0$:

$$\sin^2\theta_{13} = 0.013^{+0.007}_{-0.005}\,, \quad \Delta\chi^2 = 10.1\,(3.2\sigma) \qquad \text{(normal)},$$
$$\sin^2\theta_{13} = 0.016^{+0.008}_{-0.006}\,, \quad \Delta\chi^2 = 10.1\,(3.2\sigma) \qquad \text{(inverted)}. \tag{6}$$

As expected, the upper bound on $\sin^2\theta_{13}$ is dominated by global data without long-baseline appearance data, whereas the lower bound comes mainly from T2K.

Recently, preliminary results from the DoubleChooz reactor experiment have been presented [14], based on data taken only with the far-detector at about 1 km from 13 April to 18 September 2011 (101.5 days). A weak indication for $\bar{\nu}_e$ disappearance is observed, leading to $\sin^2 2\theta_{13} = 0.085 \pm 0.051$, which is non-zero at the 1.7σ level. In figure 5 we show the $\Delta\chi^2$ from DoubleChooz compared to the information from T2K, MINOS, and CHOOZ. We observe that the upper bound from DoubleChooz is actually slightly weaker than the CHOOZ bound, whereas the lower bound is dominated by T2K. However, again

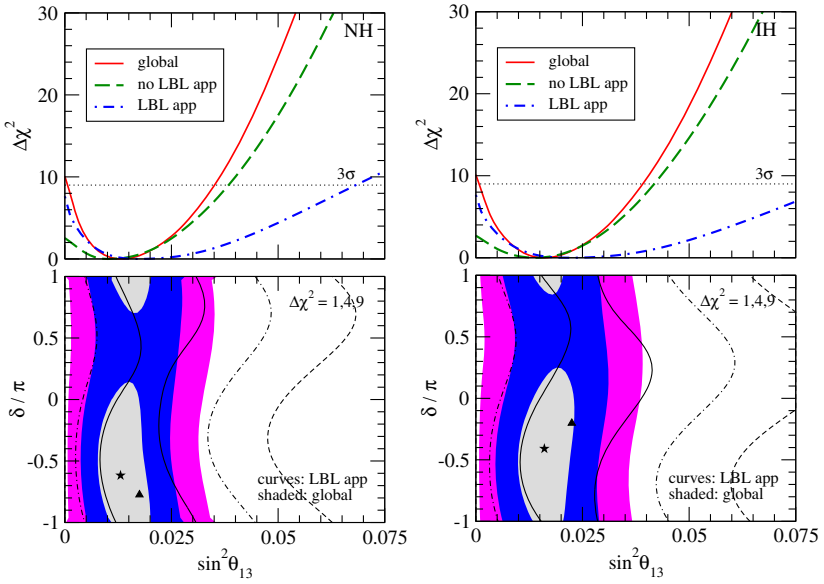

Figure 4. *Upper panels*: $\Delta\chi^2$ as a function of $\sin^2\theta_{13}$ for T2K and MINOS ν_e appearance data ('LBL app'), all the other global data ('no LBL app'), and the combined global data ('global'). *Lower panels*: contours of $\Delta\chi^2 = 1, 4, 9$ in the $\sin^2\theta_{13}$–δ plane for 'LBL app' (curves) and for the global data (shaded regions). We minimize over all undisplayed oscillation parameters. Left (right) panels are for normal (inverted) neutrino mass hierarchy. The triangle (star) corresponds to the best-fit point of the LBL app (global) analysis.

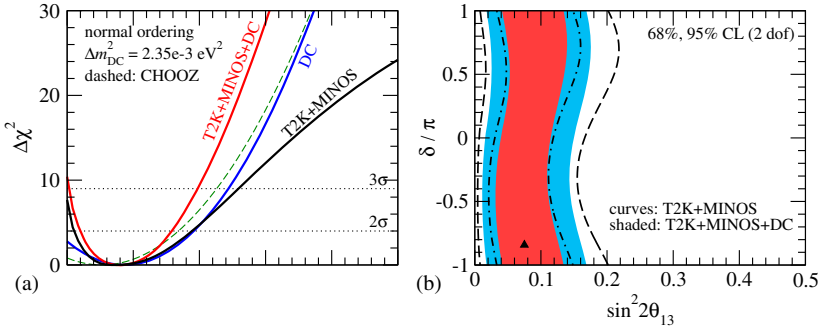

Figure 5. (**a**) $\Delta\chi^2$ from T2K+MINOS, DoubleChooz (DC), CHOOZ, and the combination T2K+MINOS+DoubleChooz. The χ^2 from T2K and MINOS is marginalized over the CP phase δ. (**b**) Regions in the plane of $\sin^2 2\theta_{13}$ and δ from T2K+MINOS (black curves) and from T2K+MINO+DoubleChooz (shaded/coloured regions).

one finds that the combined analysis leads to a value of θ_{13} being non-zero at slightly more than 3σ.

In the very near future, the experiments DayaBay, DoubleChooz, NOvA, RENO, and T2K will improve the sensitivity significantly to θ_{13}. If θ_{13} is indeed close to the present best-fit point, it should be confirmed soon with high significance (see the discussions in refs [8,15–17].

4. The reactor anomaly and sterile neutrinos

Till recently the interpretation of neutrino oscillation searches at nuclear power plants was based on the calculations of the reactor $\bar{\nu}_e$ flux (ref. [18]). Indeed, the observed rates at all the reactor experiments performed so far at distances $L \lesssim 1$ km are consistent with these fluxes thereby setting limits on $\bar{\nu}_e$ disappearance. Recently, the flux of $\bar{\nu}_e$ emitted from nuclear power plants has been re-evaluated [19], yielding roughly 3% higher neutrino fluxes than assumed previously. These increased fluxes were confirmed by an independent calculation [20]. This might indicate an anomaly in reactor experiments at $L \lesssim 1$ km, which according to the new fluxes observe a slight deficit [21]. For the CHOOZ and Palo Verde experiments at $L \simeq 1$ km a non-zero θ_{13} could lead to $\bar{\nu}_e$ disappearance accounting for the reduction of the rate. However, Δm^2_{13} and θ_{13}-driven oscillations will have no effect in short-baseline (SBL) experiments with $L \lesssim 100$ m. A flux reduction at such short baselines might be the manifestation of oscillations with sterile neutrinos at the eV mass scale [21]. We provide here an update of a global fit including LSND, MiniBooNE, and other SBL data in terms of 3+1 and 3+2 sterile neutrino mass schemes.

SBL reactor data are summarized in figure 6 (see ref. [5] for details and references). We show the observed rate relative to the predicted rate based on old and new flux calculations. Due to the slightly higher flux prediction [19], all experiments observe a smaller ratio with the new fluxes. In figure 6 we show also the result of a fit to the data with the predicted fluxes, allowing the four neutrino fluxes to float in the fit subject to systematic uncertainties. We obtain $\chi^2 = 8.1(13.0)$ for 12 degrees of freedom using old(new) fluxes. Clearly old fluxes provide a better fit to the data, whereas the χ^2 for new fluxes is still acceptable (P-value of 37%). Such a good fit can be obtained by a rescaling of the fluxes (subject to systematic uncertainties) as shown in the right panel.

The dashed lines in the figure correspond to a fit where we introduce an overall factor f in front of the fluxes, which we let float freely in the fit. For the old fluxes we find the best-fit value of $f = 0.984$ with $f = 1$ within the 1σ range. In contrast, for new fluxes we obtain $f = 0.942 \pm 0.024$, and $f = 1$ disfavoured with $\Delta\chi^2 = 6.2$ which corresponds to about 2.5σ. This is the origin of the 'reactor antineutrino anomaly' [21]. We adopt now the hypothesis that the observed deficit of SBL reactor experiments (when interpreted using the new flux predictions) is a manifestation of $\bar{\nu}_e$ disappearance induced by sterile neutrinos at the eV scale. This is particularly intriguing because the long-standing 'LSND anomaly', as well as the more recent MiniBooNE antineutrino results suggest the existence of a sterile neutrino in that mass range. Here we report on an updated analysis assuming one (3+1) or two (3+2) sterile neutrinos in light of the new reactor fluxes [22].

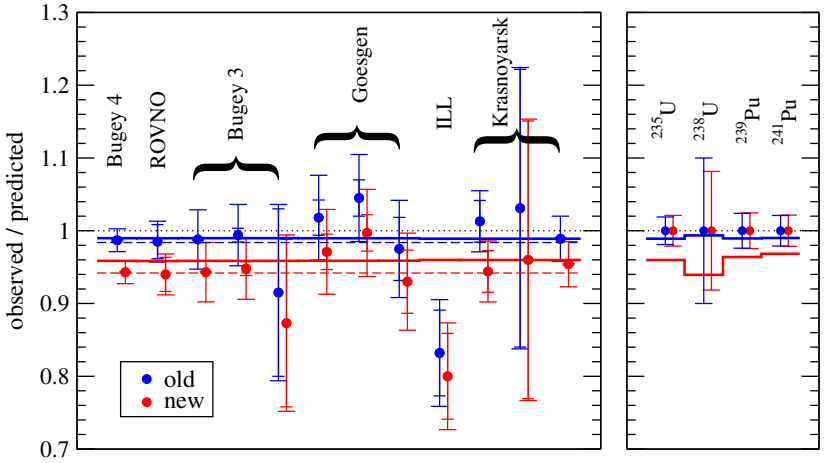

Figure 6. Short-baseline reactor data. We show the observed rate relative to the predicted rate based on old [18] and new [19,21] flux calculations. The solid histograms correspond to the fitted prediction shifted due to the uncertainty on the fluxes [21], as indicated in the right panel. The dashed lines show the best-fit assuming a free overall normalization of reactor fluxes.

Let us first discuss the implications of the new reactor antineutrino flux prediction for reactor data alone by analysing a set of SBL reactor experiments at baselines $L \lesssim 100$ m within the sterile neutrino hypothesis (for technical details see [5,22]). Within the 3+1 and 3+2 sterile neutrino frameworks, neutrino oscillations for the SBL reactor experiments depend on two and four parameters, respectively. The parameters are the mass-squared differences Δm^2_{41} and Δm^2_{51} between the eV-scale sterile neutrinos and the light neutrinos, and the elements $|U_{e4}|$ and $|U_{e5}|$ of the leptonic mixing matrix, which describe the mixing of the electron neutrino flavour with the heavy neutrino mass states ν_4 and ν_5. Obviously, for the 3+1 case, only ν_4 is present. The best-fit points for the two scenarios are summarized in table 2. The fit is dominated by Bugey3 spectral data at 15 m and 40 m and the precise rate measurement from Bugey4.

In figure 7b we show the χ^2 of the SBL reactor fit as a function of Δm^2_{41}. Using the new flux predictions (solid curves) we find a clear preference for sterile neutrino oscillations: the $\Delta\chi^2$ between the no-oscillation hypothesis and the 3+1 best-fit point is 8.5, which implies that the no-oscillation case is disfavoured at about 98.6% CL (2 DOF). In the 3+2

Table 2. Best-fit points for the 3+1 and 3+2 scenarios from reactor antineutrino data. The total number of data points is 69 (Bugey3 spectra plus 9 SBL rate measurements). For no oscillations we have $\chi^2/\text{DOF} = 59.0/69$.

	Δm^2_{41} (eV^2)	$\lvert U_{e4}\rvert$	Δm^2_{51} (eV^2)	$\lvert U_{e5}\rvert$	χ^2/DOF
3+1	1.78	0.151			50.1/67
3+2	0.46	0.108	0.89	0.124	46.5/65

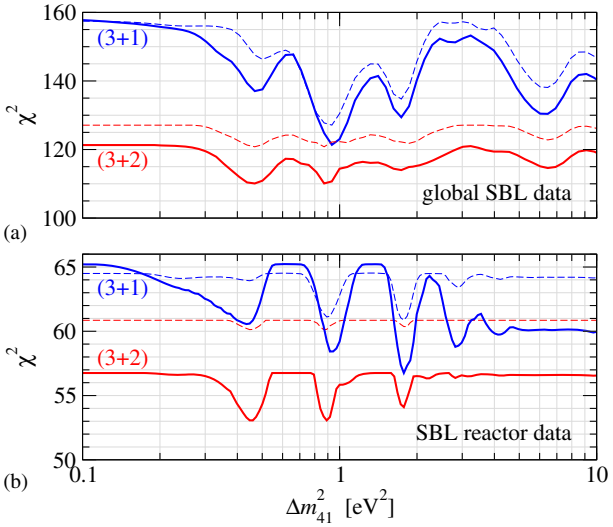

Figure 7. χ^2 from global SBL data (**a**) and from SBL reactor data alone (**b**) for the 3+1 and 3+2 scenarios. Dashed curves were computed using the old reactor antineutrino flux prediction [18], solid curves are for the new one [19]. All undisplayed parameters are minimized over. The total number of data points is 137 (84) for the global (reactor) analysis.

case the no-oscillation hypothesis is disfavoured compared to the 3+2 best-fit point with $\Delta\chi^2 = 12.1$, or 98.3% CL (4 DOF). In contrast, with previous flux predictions (dashed curves) the improvement of the fit is not significant, with a $\Delta\chi^2$ between the best-fit points and the no-oscillation case of only 3.6 and 4.4 for the 3+1 and 3+2 hypotheses, respectively.

5. Global data and the status of eV-scale sterile neutrinos

The constraints from the reactor experiments under discussion play an important role in a combined analysis of all SBL oscillation data, including the LSND and MiniBooNE anomalies. LSND has provided evidence for $\bar{\nu}_\mu \to \bar{\nu}_e$ transitions [23], which are consistent with MiniBooNE antineutrino data. This hint for oscillations are however not confirmed by a MiniBooNE search in the $\nu_\mu \to \nu_e$ channel, where the data in the energy range sensitive to oscillations are consistent with the background expectation [24]. These results seem to suggest an explanation involving CP violation in order to reconcile different results for neutrino and antineutrino searches. An explanation of the LSND and MiniBooNE anomalies via sterile neutrino oscillations requires the mixing matrix elements $|U_{e4}|$ and/or $|U_{e5}|$ to be non-zero. Reactor experiments are sensitive to these parameters, and while analyses using previous flux predictions lead to tight constraints on them, the new fluxes imply non-zero best-fit values (table 2) and closed allowed regions at 98% CL. Hence, the interesting question arises whether a consistent description of the

global data on SBL oscillations (including LSND/MiniBooNE) becomes now possible. We report here on a global fit [22] of SBL data addressing this question.

In the 3+1 scheme the SBL experiments depend on the three parameters Δm^2_{41}, $|U_{e4}|$, and $|U_{\mu 4}|$. Since only one mass scale is relevant in this case, it is not possible to obtain CP violation. Therefore, oscillations involving one sterile neutrino are not capable of reconciling the different results for neutrino (MiniBooNE) and antineutrino (LSND and MiniBooNE) appearance searches. Figure 8a compares the allowed regions from LSND and MiniBooNE antineutrino data to the constraints from the other experiments in the 3+1 model. Note that, even though reactor analyses using the new flux prediction prefer non-zero U_{e4}, no closed region appears for the disappearance bound (solid curve), since $\sin^2 2\theta_{\rm SBL} = 4|U_{e4}|^2|U_{\mu 4}|^2$ can still become zero if $U_{\mu 4} = 0$. We find that the parameter region favoured by LSND and MiniBooNE antineutrino data is ruled out by other experiments, except for a tiny overlap of the three 99% CL contours around $\Delta m^2_{41} \approx 1\,{\rm eV}^2$. Note that in this region the constraint from disappearance data does not change significantly due to the new reactor flux predictions. Using the PG test [25] we find a compatibility of the LSND+MiniBooNE($\bar{\nu}$) signal with the rest of the data only of about 10^{-5}, with $\chi^2_{\rm PG} = 21.5(24.2)$ for new(old) reactor fluxes. Hence we conclude that the 3+1 scenario does not provide a satisfactory description of the data despite the new hint coming from reactors.

Let us move now to the 3+2 model, where SBL experiments depend on the seven parameters listed in table 3. In addition to the two mass-squared differences and the moduli of the mixing matrix elements, a physical complex phase also enters,

$$\delta \equiv \arg(U_{\mu 4} U^*_{e4} U^*_{\mu 5} U_{e5})\,. \tag{7}$$

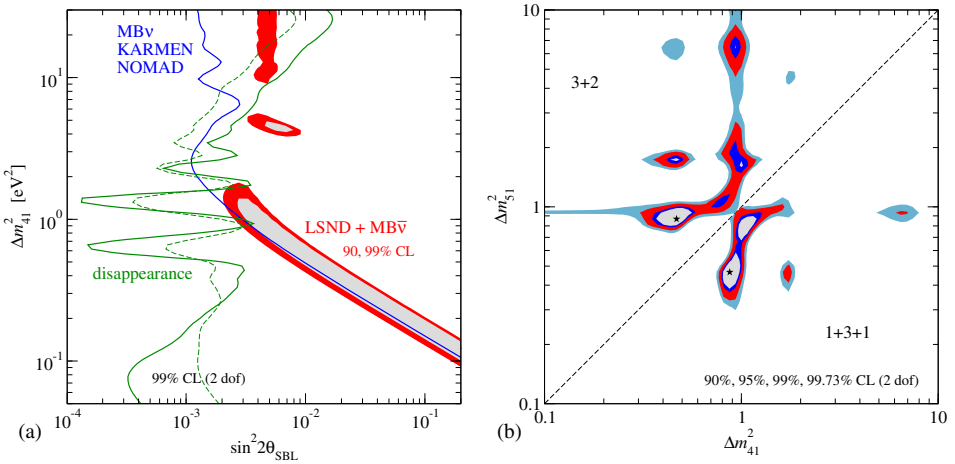

Figure 8. (**a**) Global constraints on sterile neutrinos in the 3+1 model. We show the allowed regions from LSND + MiniBooNE antineutrino vs. the constraints from null result appearance and disappearance searches. For the latter we compare the limit for the new (solid) and old (dashed) antineutrino flux prediction. (**b**) The globally preferred regions for the neutrino mass squared differences Δm^2_{41} and Δm^2_{51} in the 3+2 (upper left) and 1+3+1 (lower right) scenarios.

Table 3. Parameter values and χ^2 at the global best-fit points for 3+2 and 1+3+1 models (Δm^2's in eV^2).

	Δm^2_{41}	$\lvert U_{e4}\rvert$	$\lvert U_{\mu 4}\rvert$	Δm^2_{51}	$\lvert U_{e5}\rvert$	$\lvert U_{\mu 5}\rvert$	δ/π	χ^2/DOF
3+2	0.47	0.128	0.165	0.87	0.138	0.148	1.64	110.1/130
1+3+1	0.47	0.129	0.154	0.87	0.142	0.163	0.35	106.1/130

This phase leads to CP violation in SBL oscillations [26,27], allowing to reconcile differing neutrino and antineutrino results from MiniBooNE/LSND. Table 3 shows the parameter values at the global best-fit point and the corresponding χ^2 value. Changing from the previous to the new reactor flux calculations the χ^2 decreases by 10.6 units, indicating a significant improvement of the description of the data (see also figure 7a). From that figure it follows also that going from 3+1 to 3+2 leads to a significant improvement of the fit with the new reactor fluxes, which was not the case with the old ones. The χ^2 improves by 11.2 units, which means that 3+1 is disfavoured at the 97.6% CL (4 DOF) with respect to 3+2, compared to $\Delta\chi^2 = 6.3$ (82% CL) for old fluxes.

Figure 9 shows the predicted spectra for MiniBooNE neutrino and antineutrino data, as well as the LSND $\bar{\nu}_\mu \to \bar{\nu}_e$ transition probability. Again we find an acceptable fit to the data, although in this case the fit is slightly worse than a fit to appearance data only (dashed histograms). Note that MiniBooNE observes an event excess in the lower part of the spectrum. This excess can be explained if only the appearance data are considered, but not in the global analysis including disappearance searches [26]. In table 4 we show the compatibility of the LSND/MiniBooNE($\bar{\nu}$) signal with the rest of the data, as well as the compatibility of appearance and disappearance searches using the PG test [25]. Although the compatibility improves drastically when changing from old to new reactor fluxes, the PG is still below 1% for 3+2. This indicates that some tension between datasets remains. We considered also a '1+3+1' scenario, in which one of the sterile mass eigenstates is

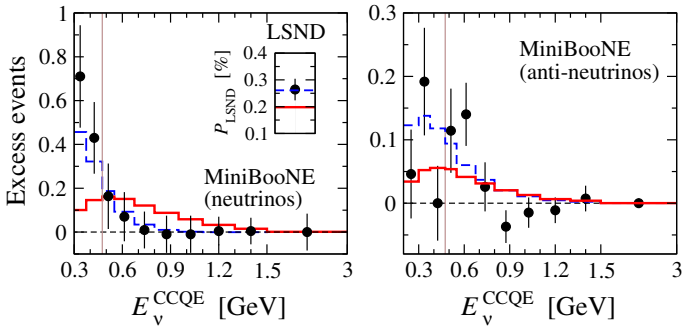

Figure 9. Predicted spectra for MiniBooNE data and the transition probability for LSND (inset). Solid histograms refer to the 3+2 global best-fit point (table 3), dashed histograms correspond to the best-fit of appearance data only (LSND, MiniBooNE $\nu/\bar{\nu}$, KARMEN, NOMAD).

Table 4. Compatibility of datasets [25] for 3+2 and 1+3+1 using old and new reactor fluxes.

	LSND+MB($\bar{\nu}$) vs. rest		Appearance vs. disapp.	
	Old	New	Old	New
$\chi^2_{\mathrm{PG},3+2}$/DOF	25.1/5	19.9/5	19.9/4	14.7/4
PG_{3+2}	10^{-4}	0.13%	5×10^{-4}	0.53%
$\chi^2_{\mathrm{PG},1+3+1}$/DOF	19.6/5	16.0/5	14.4/4	10.6/4
PG_{1+3+1}	0.14%	0.7%	0.6%	3%

lighter than the three active ones and the other is heavier. As can be seen from tables 3 and 4 the fit of 1+3+1 is slightly better than 3+2, with $\Delta\chi^2 = 15.2$ between 3+1 and 1+3+1 (99.6% CL for 4 DOF). However, due to the larger total mass in neutrinos, a 1+3+1 ordering might be in more tension with cosmology than a 3+2 scheme [28–30]. Figure 8b shows the allowed regions for the two eV-scale mass-squared differences for the 3+2 and 1+3+1 schemes.

Let us comment briefly on other signatures of eV sterile neutrinos. We have checked the fit of solar neutrino data and the KamLAND reactor experiment, and found excellent agreement. The effect of non-zero values of U_{e4} and U_{e5} for these data are similar to the one of U_{e3} in the standard three-active neutrino case, and hence the 3+2 best-fit point mimics a non-zero U_{e3} close to the preferred value of these data. The MINOS long-baseline experiment has performed a search for sterile neutrinos via neutral current (NC) measurements. We have estimated that the best-fit points reported in table 3 lead to an increase of the χ^2 of MINOS NC data as well as χ^2_{PG} by a few units. Radioactive source measurements in gallium solar neutrino experiments report an event deficit which could be a manifestation of electron neutrino disappearance due to eV-scale sterile neutrinos [31]. Our best-fit points fall in the range of parameter values capable to explain these data [31]. Finally, eV-scale sterile neutrinos may manifest themselves in cosmology. Recent studies [28–30] indicate a slight preference for extra radiation content in the Universe (mainly from CMB measurements), favouring the existence of light sterile neutrinos. On the other hand, Big-Bang nucleosynthesis leads to an upper bound on the number of extra neutrino species of 1.2 at 95% CL [32], which may be a challenge for two-sterile neutrino schemes. Moreover, global fits to cosmological data constrain the sum of the neutrino masses to be less than 0.7 to 1.5 eV at 95% CL [28–30], depending on the used data, whereas our 3+2 best-fit point leads to $\sum m_\nu \approx 1.7$ eV. Hence, sterile neutrino explanations of short-baseline oscillation data are in tension with cosmology, or, if confirmed, would indicate a deviation from the standard cosmological picture.

6. Conclusions

We have presented an update of the global status of neutrino oscillation data. The bulk of the global data can be described within the three-flavours of the Standard Model, and a rough picture of lepton mixing has emerged. Dominant oscillation modes are measured

with increasing precision. Moreover, we have hints that the last unknown mixing angle θ_{13} is not so far from the current upper bound. First results from T2K indicate a non-zero value, consistent with the global data as well as preliminary results from DoubleChooz. Global analyses lead to θ_{13} being non-zero at the 3σ level.

There are a few anomalies which cannot be explained within the three-flavour picture, and might point towards sterile neutrinos at the eV scale. This is the long-standing LSND puzzle, as well as a recent re-evaluation of the neutrino flux from nuclear reactors, which lead to the so-called reactor anomaly. Indeed, a global fit to short-baseline oscillation searches assuming two sterile neutrinos improves significantly when new predictions for the reactor neutrino flux are taken into account. However, significant tension remains in the global fit due to a conflict between appearance and disappearance searches. Although we are facing an intriguing accumulation of hints for the existence of sterile neutrinos at the eV scale, the situation is inconclusive and no coherent picture has emerged so far.

Acknowledgements

The author would like to acknowledge the financial support of the European Community under the European Commission Framework Programme 7 Design Study: EUROnu, Project Number 212372. The EC is not liable for any use that may be made of the information contained herein.

References

[1] Z Maki, M Nakagawa and S Sakata, *Prog. Theor. Phys.* **28**, 870 (1962)
B Pontecorvo, *Zh. Eksp. Theor. Fiz.* **53**, 1717 (1967) [*Sov. Phys. JETP* **26**, 984 (1968)]
[2] Particle Data Group: K Nakamura *et al*, *J. Phys.* **G37**, 075021 (2010)
[3] K Zuber, *These proceedings*
[4] T Schwetz, M Tortola and J W F Valle, *New J. Phys.* **10**, 113011 (2008), arXiv:0808.2016
[5] T Schwetz, M Tortola and J W F Valle, *New J. Phys.* **13**, 063004 (2011), arXiv:1103.0734
[6] T Schwetz, M Tortola and J W F Valle, *New J. Phys.* **13**, 109401 (2011), arXiv:1108.1376
[7] A Gando *et al*, *Phys. Rev.* **D83**, 052002 (2011), arXiv:1009.4771
[8] J Thomas, *These proceedings*
[9] The MINOS Collaboration: P Adamson *et al*, *Phys. Rev. Lett.* **106**, 181801 (2011), arXiv:1103.0340
[10] CHOOZ: M Apollonio *et al*, *Eur. Phys. J.* **C27**, 331 (2003), hep-ex/0301017
[11] H Tanaka, *These proceedings*
[12] T2K Collaboration: K Abe *et al*, *Phys. Rev. Lett.* **107**, 041801 (2011), arXiv:1106.2822
[13] MINOS Collaboration: P Adamson *et al*, *Phys. Rev. Lett.* **107**, 181802 (2011), arXiv:1108.0015
[13a] Prospects to constrain δ with the present generation of experiments are discussed in ref. [15].
[14] H deKerret, talk at the LowNu Conference (Korea, 11 Nov. 2011)
[15] P Huber, M Lindner, T Schwetz and W Winter, *J. High Energy Phys.* **11**, 044 (2009), arXiv:0907.1896
[16] M Mezzetto and T Schwetz, *J. Phys.* **G37**, 103001 (2010), arXiv:1003.5800
[17] K-B Luk, *These proceedings*

[18] K Schreckenbach, G Colvin, W Gelletly *et al*, *Phys. Lett.* **B160**, 325 (1985)
A A Hahn, K Schreckenbach, G Colvin *et al*, *Phys. Lett.* **B218**, 365 (1989)
F Von Feilitzsch, A A Hahn and K Schreckenbach, *Phys. Lett.* **B118**, 162 (1982)
P Vogel, G K Schenter, F M Mann *et al*, *Phys. Rev.* **C24**, 1543 (1981)
[19] T A Mueller *et al*, *Phys. Rev.* **C83**, 054615 (2011), 1101.2663
[20] P Huber, *Phys. Rev.* **C84**, 024617 (2011), arXiv:1106.0687
[21] G Mention *et al*, *Phys. Rev.* **D83**, 073006 (2011), 1101.2755
[22] J Kopp, M Maltoni and T Schwetz, *Phys. Rev. Lett.* **107**, 091801 (2011), arXiv:1103.4570
[23] LSND: A Aguilar *et al*, *Phys. Rev.* **D64**, 112007 (2001), hep-ex/0104049
[24] MiniBooNE: A A Aguilar-Arevalo *et al*, *Phys. Rev. Lett.* **98**, 231801 (2007), arXiv:0704.1500
[25] M Maltoni and T Schwetz, *Phys. Rev.* **D68**, 033020 (2003), hep-ph/0304176
[26] M Maltoni and T Schwetz, *Phys. Rev.* **D76**, 093005 (2007), 0705.0107
[27] G Karagiorgi *et al*, *Phys. Rev.* **D75**, 013011 (2007), Erratum, *ibid.* **D80**, 099902 (2009), hep-ph/0609177
[28] M C Gonzalez-Garcia, M Maltoni and J Salvado, *J. High Energy Phys.* **1008**, 117 (2010), 1006.3795
[29] J Hamann *et al*, *Phys. Rev. Lett.* **105**, 181301 (2010), 1006.5276
[30] E Giusarma *et al*, *Phys. Rev.* **D83**, 115023 (2011), 1102.4774
[31] M A Acero, C Giunti and M Laveder, *Phys. Rev.* **D78**, 073009 (2008), 0711.4222
[32] G Mangano and P D Serpico, *Phys. Lett.* **B701**, 296 (2011), 1103.1261